LIMITATIONS TO SENSING OF WEB TENSION BY MEANS OF ROLLER REACTION FORCES

by

J. J. Shelton
Oklahoma State University
USA

ABSTRACT

Classical frequency response analysis of a dancer or a roller mounted on load cells reveals that such devices are severely limited in their ability to sense the dynamic tension in a web. The response of a tension control system may therefore be limited by the dynamics of the sensor instead of the drive motor and its controller.

Natural frequencies of rollers in translation and rotation are shown to limit the bandwidth of tension control systems. Dancers are shown to often increase dynamic tension variations when compared to a simple span of web, instead of performing their intended function of reducing or eliminating these variations.

Transfer functions of web dynamics reveal that a tension control system may appear to be one "type" (as defined by the number of pure integrations in the open loop), but the tension output does not benefit from the integrations, yet the control system suffers the difficulty of stabilization associated with integration(s). A dancer which controls a torque device (contrasted with control of velocity) is particularly difficult to stabilize because of the double integration (type 2) and the great variations of important parameters.

Dimensionless groups of parameters were developed for evaluation of the performance of roller-reaction sensors of tension. Performance is shown to depend upon the stiffness and velocity of the web, as well as such parameters of machine design as the number of the idlers between the driven rollers, mass and radius of each roller, stiffness of the load cells, and lengths of spans between drive stations. A subgroup of parameters (not dimensionless) is the inertia of a roller divided by the square of its radius. Because this subgroup is never separated into its two components, the inertia by itself is unimportant.

NOMENCLATURE

A	the span between the controlled roll or roller and the sensing roller
A	the first idler in a series and its entering span (multiple idlers)
B	the span across the sensing roller from the controlled roll or roller
B	the second idler in a series and its entering span (multiple idlers)
C	damping constant of a dancer or load cell
C	the third idler in a series and its entering span (multiple idlers)
C_n	constant for expressing the undamped natural frequency
D	the exiting span from the third idler in a series (multiple idlers)
E	tensile modulus of elasticity of the web in the longitudinal direction
J	mass moment of inertia
j	$\sqrt{-1}$
K	total spring rate of a dancer or set of load cells
L	length of a span
L_T	total length of spans between driven rollers
m	effective translational mass of a roll or roller
R	a constant radius
r	a variable radius
s	Laplacian operator (equal to $j\omega$ for frequency response analysis)
T	web tension
T	torque
t	web thickness
V	web velocity
W	web width
Y	dancer displacement
Δ	amplitude of the sinusoidal change from the average condition
θ	angle of wrap (radians)
τ	time constant (seconds) of a web span (the time for traveling through the span)
ω	frequency or rotational velocity (radians per second)

Subscripts

A,B,C,D	pertaining to Spans A, B, C, and D, respectively
i	"initial" condition (the average about which sinusoidal deviation occurs)
N	pertaining to the downstream driven roller (multiple idlers)
o	pertaining to the unwinding or winding roll
o	pertaining to the upstream driven roller (multiple idlers)
V	pertaining to the velocity control
1	pertaining to the dancer roller

INTRODUCTION

The signal for automatic control of the tension on a moving web is usually obtained from load cells which support a roller wrapped by the web, or from the position of a force-balanced floating roller ("dancer"). The dynamic response of such devices is severely limited because of the massiveness of rollers, as required for economy and practicality of fabrication and operation. The dynamic response may be further worsened by interaction between the sensing roller and neighboring idlers,

particularly if the friction between the web and these idlers is high. If the performance of a tension control system is limited by the sensor, expense and effort would be wasted in improvement of the response of other components.

This paper is aimed at feedback control of tension, particularly when the velocity of a transport roller is the controlled variable of an inner loop. Papermaking machines and other process lines where tension is controlled by the velocities of the driven rollers without sensing of the tension, are therefore not considered, nor are process lines in which torque is the controlled variable. Control of torque is commonly employed for indirect control of tension in simple process lines (slitters, for example) and in lines for processing metals, where the stiffness of the web may be so great that its variability does not significantly affect the tension. Control of tension by means of precise control of velocity, however, allows independent control of zones without steady-state interaction, and minimizes the effects of external disturbances; furthermore, control of velocity is becoming less expensive and more precise with advances in digital control equipment.

The length of web in contact with a roller is assumed to be negligible in comparison to the length of spans on either side of the roller. The length of wrap on a *drive* roller or the total length of web in a closely spaced cluster of synchronized *drive* rollers is of little importance in automatic control of velocity-controlled tension, as a disturbance in tension (strain) is merely delayed in its transport from one tension zone to the next, with no delay within a control loop. In contrast, a significant length of web in contact with an *idler* modifies the dynamics of this report; however, the complexity of the dynamics of partial slippage is immense.

Velocity control may be applied to devices other than rollers. For example, the tension of a web feeding into a tenter or onto a vacuum belt may be controlled by controlling the velocity of the tenter or belt.

Classical methods of frequency response analysis were applied in this study. The governing differential equations were written and linearized, then the Laplace transformation was applied to obtain algebraic equations in powers of the Laplacian operator "s". These equations were combined, then solved for the output(s) in terms of the input(s). The operator s was then replaced with $j\omega$, allowing the relation between the output and input amplitude and phase angle to be obtained at each frequency of the sinusoidal input.

Zero friction between the web and roller was modeled by assuming zero inertia but using the true mass for translation, a subterfuge which is physically impossible but is legitimate for modeling.

For the common case of a disturbance to tension caused by an eccentric unwinding roll (which results in one approximately sinusoidal cycle per revolution), the usual nondimensionalized frequency $\omega\tau$ can be replaced by its equivalent $(V_i/r_{oi})(L/V_i) = L/r_{oi}$. Frequency then does not have to be calculated as a function of velocity, and the response may be expressed as a function of parameters of the process line and the web, and the velocity of the web.

Because the behavior of a function of a complex variable is seldom obvious, this report depends heavily on graphs for presentation of results. Allowing space for

enough graphs to portray the results required omission of details of derivations as well as unsimplified versions of transfer functions, which are very lengthy in some cases.

GOVERNING EQUATIONS

For an angular-velocity-controlled unwinder as shown in Figure 1, the linearized change of velocity of the web as it leaves the unwinding roll, with the change of radius as a disturbance, is

$$\Delta V_o = \omega_{oi}\Delta r_o + r_{oi}\Delta\omega_o. \tag{1}$$

The other unknown variables ΔV_1, ΔT_A, ΔT_B, and Δy must be determined by four equations, (1) the continuity equation for span A, (2) the continuity equation for span B, (3) the equation for angular acceleration of the roller, and (4) the equation for translational acceleration of the roller:

$$\begin{bmatrix} 1 & 0 & 0 & 0 & 0 \\ -1 & 1 & -\left(\frac{L_{Ai}s+V_i}{EtW}\right) & 0 & s \\ 0 & -1 & \frac{V_i}{EtW} & -\left(\frac{L_{Bi}s+V_i}{EtW}\right) & s \\ 0 & -\left(\frac{J_1}{R_1^2}\right)s & -1 & 1 & 0 \\ 0 & 0 & 1 & 1 & m_1s^2+C_1s+K_1 \end{bmatrix} \begin{bmatrix} \Delta V_o(s) \\ \Delta V_1(s) \\ \Delta T_A(s) \\ \Delta T_B(s) \\ \Delta Y(s) \end{bmatrix}$$

$$= \begin{bmatrix} \frac{V_i}{r_{oi}}\Delta r_o(s)+r_{oi}\Delta\omega_o(s) \\ -\frac{V_i}{EtW}\Delta T_o(s) \\ 0 \\ 0 \\ \Delta F(s) \end{bmatrix}. \tag{2}$$

The independent variables in equation (2) are the change in radius, Δr_o, the change in the wound-in tension, ΔT_o, the change in the bias force on the dancer, ΔF, and the change in the angular velocity, $\Delta\omega_o$.

If torque instead of velocity of the unwinding roll is controlled, as by a simple brake or a current-controlled motor, the change in angular velocity of the spindle, $\Delta\omega_o$, as well as the change of velocity of the web as it leaves the wound roll, ΔV_o, become dependent variables:

$$\begin{bmatrix} -r_{0i} & 1 & 0 & 0 & 0 & 0 \\ 0 & -1 & 1 & -\frac{L_{Ai}s+V_i}{EtW} & 0 & s \\ 0 & 0 & -1 & \frac{V_i}{EtW} & -\frac{L_{Bi}s+V_i}{EtW} & s \\ -J_o s & 0 & 0 & r_{01} & 0 & 0 \\ 0 & 0 & -\frac{J_1}{R_1^2}s & -1 & 1 & 0 \\ 0 & 0 & 0 & 1 & 1 & m_1s^2+C_1s+K_1 \end{bmatrix} \begin{bmatrix} \Delta\omega_o(s) \\ \Delta V_0(s) \\ \Delta V_1(s) \\ \Delta T_A(s) \\ \Delta T_B(s) \\ \Delta Y(s) \end{bmatrix}$$

$$= \begin{bmatrix} \frac{V_i}{r_{oi}}\Delta r_o(s) \\ -\frac{V_i}{EtW}\Delta T_o(s) \\ 0 \\ \Delta T_o(s) - T_{Ai}\Delta r_o(s) \\ 0 \\ \Delta F(s) \end{bmatrix}. \tag{3}$$

The first row in the above 6 x 6 matrix represents the linear velocity of the web as it leaves the roll as a function of the changing radius and the changing angular velocity. The second and third rows are the continuity equations for spans A and B, while the fifth and sixth rows are the equations for angular and translational accelerations of the roller, as for the case of the velocity-controlled unwinder. The fourth row represents the angular acceleration of the unwinding roll as a function of the summation of imposed torques.

The winder of Figure 2 has its parameters labeled for similarity to the unwinder; however, the two tension-control stations are not identical because of the reversal of the transport of strain, as well as a reversal of signs for the tensions causing angular acceleration of the roller. For an angular-velocity-controlled winder:

$$\begin{bmatrix} 1 & 0 & 0 & 0 & 0 \\ 0 & 1 & 0 & -\left(\frac{L_{Bi}s+V_i}{EtW}\right) & s \\ 1 & -1 & \left(\frac{L_{Ai}s+V_i}{EtW}\right) & \frac{V_i}{EtW} & s \\ 0 & -\frac{J_1}{R_1^2}s & 1 & -1 & 0 \\ 0 & 0 & 1 & 1 & m_1s^2+C_1s+K_1 \end{bmatrix} \begin{bmatrix} \Delta V_o(s) \\ \Delta V_1(s) \\ \Delta T_A(s) \\ \Delta T_B(s) \\ \Delta Y(s) \end{bmatrix}$$

$$= \begin{bmatrix} \frac{V_i}{r_{oi}}\Delta r_o(s) + r_{oi}\Delta\omega_o(s) \\ \Delta V_2(s) - \frac{V_i}{EtW}\Delta T_c(s) \\ 0 \\ 0 \\ \Delta F(s) \end{bmatrix}. \tag{4}$$

The last subsystem to be studied is one, two, or three neighboring idlers which are rigidly mounted and infinitely stiff and which have no dynamic slippage relative

to the web. The assumption of infinite stiffness is not unrealistic if the translational natural frequency of each roller, one of which might be mounted on stiff load cells, is several times higher than the lowest calculated rotational natural frequency. The assumption of zero dynamic slippage is commonly unrealistic for a high-speed, non-permeable web, but represents the worst dynamics which can be inflicted by friction, which is highly variable and poorly predictable. This subsystem is shown in Figure 3, with one idler on load cells as an example.

The equations governing the behavior of three successive idlers are four continuity equations for the four spans and three equations of angular acceleration of the three rollers:

$$\begin{bmatrix} \frac{L_A s + V_i}{EtW} & -1 & 0 & 0 & 0 & 0 & 0 \\ -\frac{V_i}{EtW} & 1 & \frac{L_B s + V_i}{EtW} & -1 & 0 & 0 & 0 \\ -1 & -\frac{J_A}{R_A^2} s & 1 & 0 & 0 & 0 & 0 \\ 0 & 0 & -\frac{V_i}{EtW} & 1 & \frac{L_C s + V_i}{EtW} & -1 & 0 \\ 0 & 0 & -1 & -\frac{J_B}{R_B^2} s & 1 & 0 & 0 \\ 0 & 0 & 0 & 0 & -\frac{V_i}{EtW} & 1 & \frac{L_D s + V_i}{EtW} \\ 0 & 0 & 0 & 0 & -1 & -\frac{J_C}{R_C^2} s & 1 \end{bmatrix} \begin{bmatrix} \Delta T_A(s) \\ \Delta V_A(s) \\ \Delta T_B(s) \\ \Delta V_B(s) \\ \Delta T_C(s) \\ \Delta V_C(s) \\ \Delta T_D(s) \end{bmatrix}$$

$$= \begin{bmatrix} \frac{V_i}{EtW} \Delta T_o(s) - \Delta V_o(s) \\ 0 \\ 0 \\ 0 \\ 0 \\ \Delta V_D(s) \\ 0 \end{bmatrix}. \qquad (5)$$

NATURAL FREQUENCIES

In a control system, if mechanical backlash is avoided and if time delays (including the sampling period of a digital system) are very small, the response is usually limited by the lowest natural frequency. In a tension control system, this lowest natural frequency could be the result of a high-inertia roller which is driven through a torsionally flexible shaft or coupling; however, such a resonance usually can be raised to any desired frequency by attention to details of design. Another type of resonance which can affect control of tension is the translational natural frequency (actually, multiple frequencies) of a roller, whether a driven roller, a load-cell roller, or a simple idler. This resonance can usually be raised to a desired level by increasing the diameter of the roller, as shown by Shelton [1].

The natural frequencies considered in this study are (1) those caused by mass/spring systems consisting of a roller which is stiff enough to be considered as a concentrated mass (at the frequencies of interest) with the web and/or the mounting of

the roller acting as a spring, and (2) those caused by the rotational inertia of a roller which is gripped by the web sufficiently to vibrate rotationally, with the web acting as a spring.

If the friction between the web and roller is so low that little transient angular acceleration occurs (a common condition for high-speed, nonpermeable webs), the natural frequency of an ideal dancer (zero spring rate, no mechanical damping, and 180-degree wrap) is

$$\omega_n = 2\sqrt{\frac{EtW}{m_1 L_T}}. \tag{6}$$

For the same conditions as above, except that the roller is mounted on load cells which have a total spring rate K_1 much greater than the spring rate EtW/L_T of the web:

$$\omega_n = \sqrt{K_1 / m_1}. \tag{7}$$

If neither spring rate is large in comparison to the other, but little transient angular acceleration occurs, the natural frequency is

$$\omega_n = \sqrt{\frac{K_1}{m_1}\left[1 + 4\frac{EtW}{K_1 L_T}\right]}. \tag{8}$$

Equations (6) and (7) are clearly special cases of equation (8).

If the wrap on a load cell roller is θ (less than 180 degrees) equation (8) is modified to

$$\omega_n = \sqrt{\frac{K_1}{m_1}\left[1 + 4\frac{EtW \sin^2(\theta/2)}{m_1 L_T}\right]}. \tag{9}$$

Unless a flywheel with a diameter greater than that of the roller is added to a roller, the radius of gyration is less than the radius. Typically, J/mR^2 is approximately 0.75, but this "roller design parameter" might be lower unless the masses of shafts, bearings, and hubs, plus the effective mass of the arms and actuator of a dancer, can be kept low relative to the mass of the shell of the roller. For examples of rollers without flywheels, the translational natural frequency has been found to be unchanged from the values of equations (6) through (9) if no slippage occurs, but a higher rotational natural frequency also occurs.

For one or more rigidly mounted, identical, non-slipping idlers in a zone between driven rollers, the natural frequencies are

$$\omega_n = C_n\sqrt{\frac{R^2 EtW}{JL_T}}. \tag{10}$$

C_n is 2.000 for one idler if the entering and exiting spans are equal. The lowest natural frequency for multiple idlers with all spans equal is specified by C_n equal to 1.732 for two idlers, 1.531 for three, 1.382 for four, and 1.268 for five.

TRANSFER FUNCTIONS AND BODE PLOTS

An ideal dancer which has insufficient friction to be significantly accelerated and decelerated (angularly) by periodic velocity changes of the web exhibits the following response to the surface velocity of a velocity-controlled unwinding or winding roll:

$$\frac{\Delta T(s)}{\Delta V_o(s)} = \frac{(m_I/4)s}{\frac{L_T m_I}{4EtW}s^2 + \frac{m_I V_i}{4EtW}s + 1}, \tag{11}$$

and

$$\frac{\Delta Y(s)}{\Delta V_o(s)} = \frac{1/2}{s\left(\frac{L_T m_I}{4EtW}s^2 + \frac{m_I V_i}{4EtW}s + 1\right)}, \tag{12}$$

with a winder and unwinder differing by no more than an overall minus sign.

Note that equation (11) is a mathematical confirmation of the intuitively obvious: A periodic variation of tension, as a derivative function of velocity, has an extremely low amplitude at low frequencies. Equation (12), however, shows the displacement of the dancer, the variable used for feedback control of tension, to be an integral function of the velocity. Figures 5 and 6 are plots of equations (11) and (12).

If the dynamic spring rate K_I of a dancer is not negligible in comparison to the spring rate EtW/L_T of the web, the transfer functions corresponding to equations (11) and (12) are somewhat more complicated. Figures 7, 8, and 9 show that attenuation of the disturbance from an eccentric unwinding roll is excellent over a narrow bandwidth of frequency (or the ratio L_T/r_{oi}), but has a resonant peak at a higher frequency, where attenuation would be better if the roller were fixed.

If transient slippage does not occur, the transfer functions are again lengthy, and ΔT_A then differs from ΔT_B, as shown in Figures 10 and 11. ΔT_B is generally more important for an unwinder than ΔT_A because of the transport of strain into the process. The example curves of Figure 12 show no spectacular differences between zero slippage and total slippage. The translational resonances are at the same frequencies, but the rotational resonance appears at a higher frequency in the absence of slippage. These dual resonances also appear in Figures 10 and 11.

Figure 13 shows examples of the results of adding a flywheel to a roller with a typical value of J/mR^2 equal to 0.75 to make the radius of gyration equal to the radius, or $J/mR^2 = 1$. Only if specific operating conditions are chosen is the flywheel advantageous; in fact, the added mass is detrimental to attenuation at low frequencies.

The amplitudes are equal at the translational resonance, which is the primary deterrent to using a dancer.

For a roller mounted on load cells with 180 degrees of wrap, the model is the same as for a dancer, as shown in Figure 1 and as specified by equation (2). If the friction is negligible, equations (8) or (9) specify the natural frequency of this simple second-order system. If slippage does not occur, Figures 14 and 15 show the response in the two spans, and Figure 16 shows the relationship between the tensions in these spans. A peak in the latter figure does not occur at the same frequency as the peaks in Figures 14 and 15, but correspond to minima of ΔT_A.

If torque instead of velocity of an unwinder is controlled, as defined by equations (3), transfer functions for the case of negligible friction as in equations (11) and (12) are

$$\frac{\Delta T(s)}{\Delta T(s)} = \frac{1}{r_{oi}\left[\frac{J_o L_T}{r_{oi}^2 EtW}s^2 + \frac{J_o V_i}{r_{oi}^2 EtW}s + \left(1 + 4\frac{J_o}{r_{oi}^2 m_1}\right)\right]} \tag{13}$$

and

$$\frac{\Delta Y(s)}{\Delta T(s)} = \frac{2}{r_{oi} m_1 s^2\left[\frac{J_o L_T}{r_{oi}^2 EtW}s^2 + \frac{J_o V_i}{r_{oi}^2 EtW}s + \left(1 + 4\frac{J_o}{r_{oi}^2 m_1}\right)\right]}. \tag{14}$$

Figure 17, a plot of equation (13), shows little difference between the attenuation of tension variations caused by an eccentric unwinding roll for torque control of this graph and velocity control of Figure 5, except when the mass of the unwinding roll approaches the mass of the dancer roller. The reason for this behavior is that the rotational inertia of a massive roll keeps its rotational velocity nearly constant even when it is eccentric and unbalanced. Equation (14), however, shows that the position of the dancer roller is related to the torque by a double integration (s^2 in the denominator), making stabilization difficult when a torque device is controlled by a dancer.

The responses of one, two, or three idlers to changes in the velocity of the upstream or downstream drive roller are plotted in Figures 18 through 32. In these figures, the numbers on the curves are the values of JV_i^2/R^2L_TEtW. The solid curves are for all values of J/R^2 equal, while dashed curves are identified as other conditions. The time constant τ_T is the time for the web to travel from drive roller to drive roller (through all two, three, or four spans). Further, no slackness and no slippage are assumed.

Figures 18 through 32 show great variations in amplitude ratio and phase angle, which lags by as much as 630 degrees. However, the phase relationship is never greater than 90 degrees in the span adjacent to the input roller.

CONCLUSIONS

The dynamics of dancers and load-cell rollers, even with several simplifying assumptions, are quite complicated; furthermore, the uncertainty of web/roller friction as affected by velocity, contamination, wear, and other variables renders any prediction of dynamics questionable. The dynamic behavior is well defined only below the lowest natural frequency of a subsystem of the web and rollers. If the tension control system is designed for severe attenuation of response near and above the lowest natural frequency, the response of tension to velocity can sometimes be approximated as a first-order lag, described by Boulter and Gao [2] as "commonly used". The validity of this simple transfer function for a rigid roller on stiff load cells is also suggested by observation of the repetition of responses in Figures 18 through 32 when $\omega\tau_T$ is less than 1.0.

The graphs of Figures 5 through 32 show the usefulness of a dimensionless group of variables, the mass of a roller in translation or the inertia divided by the square of the radius of gyration in rotation, multiplied by the square of the velocity of the web, and divided by an appropriate distance and the unit stiffness EtW of the web, as an indicator of the responsiveness of a dancer or load-cell roller. Decreasing the mass of the roller may be the only improvement in this group of variables which is left to the discretion of the designer.

REFERENCES

[1] Shelton, John J., "Deflection and Critical Velocity of Rollers", Proceedings of the Third International Conference on Web Handling, Oklahoma State University, June, 1995.

[2] Boulter, Brian T., and Z. Gao, "Matrix Interpolation Based Self-Tuning Web Tension Regulation", Proceedings of the Third International Conference on Web Handling, Oklahoma State University, June, 1995.

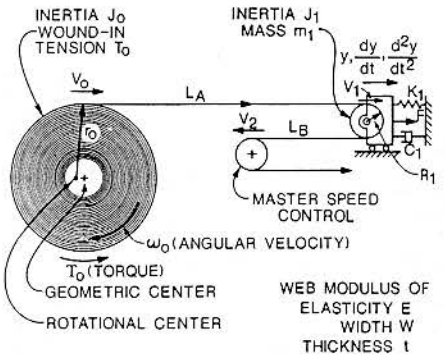

Fig. 1. Schematic of Unwinder with Dancer or Load Cell Control

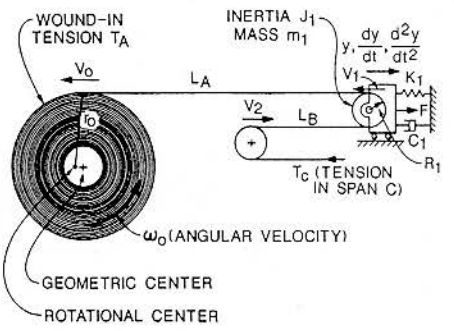

Fig. 2. Schematic of Winder with Dancer or Load Cell Control

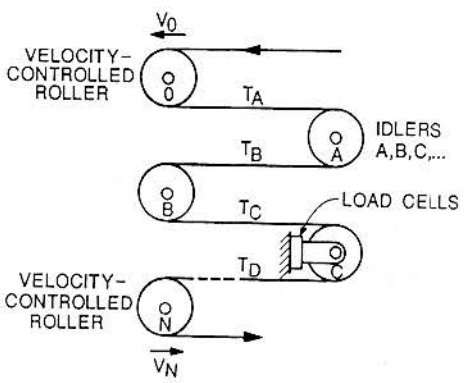

Fig. 3. One Tension-Sensing Idler and other Idlers between Driven Rollers

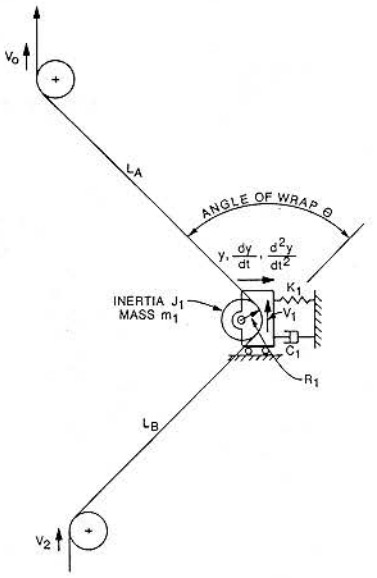

Fig. 4. Schematic of Load-Cell Idler with Equal Sensitivity to Tension in Two Spans

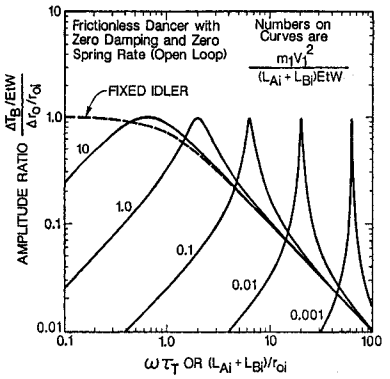

Fig. 5. Attenuation of Disturbance from Eccentricity of Unwinding or Winding Roll at Constant Angular Velocity–Frictionless Dancer

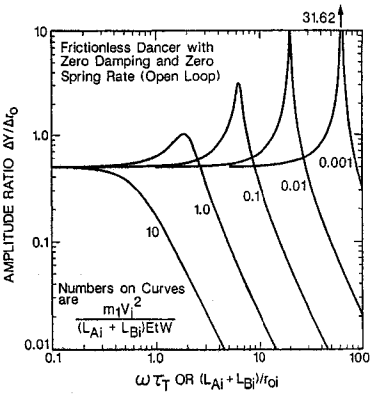

Fig. 6. Response of Dancer Position to Unwinding Roll Eccentricity – Dancer after Velocity-Controlled Unwind

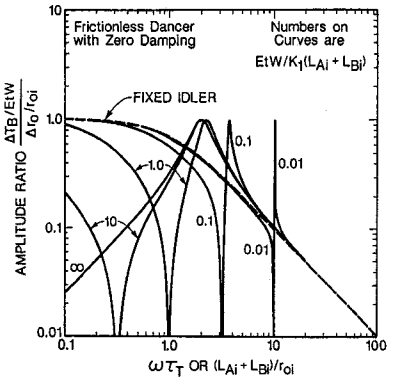

Fig. 7. Open Loop Response of Tension to Unwinding Roll Eccentricity – Dancer after Velocity-Controlled Unwind with $m_1V_i^2/(L_{Ai}+L_{Bi})$ EtW = 0.01

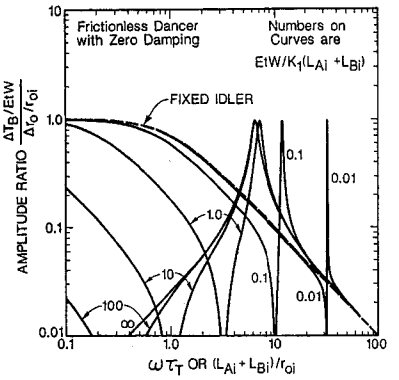

Fig. 8. Open Loop Response of Tension to Unwinding Roll Eccentricity – Dancer after Velocity-Controlled Unwind with $m_1V_i^2/(L_{Ai}+L_{Bi})$ EtW = 0.1

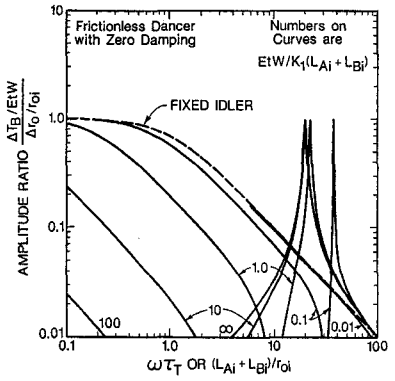

Fig. 9. Open Loop Response of Tension to Unwinding Roll Eccentricity – Dancer after Velocity-Controlled Unwind with $m_1V_i^2/(L_{Ai} + L_{Bi})$ EtW = 1.0

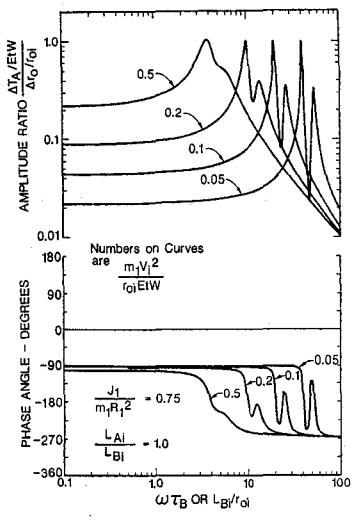

Fig. 10. Frequency Response of Span Upstream of Dancer for Velocity-Controlled Unwind with Eccentric Roll (Open Loop, No Slippage)

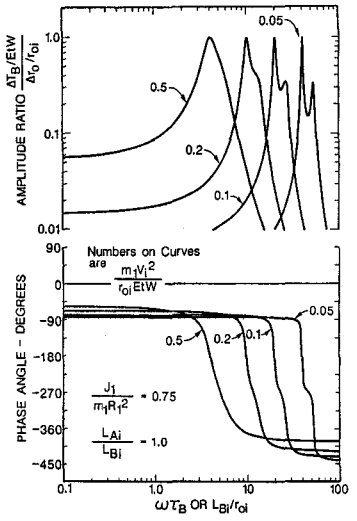

Fig. 11. Frequency Response of Span Downstream from Dancer for Velocity-Controlled Unwind with Eccentric Roll (Open Loop, No Slippage)

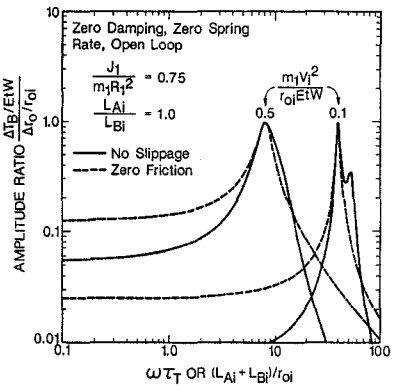

Fig. 12. Comparison of Tensions in Exiting Span for Dancer after Velocity-Controlled Unwind – with and without Slippage

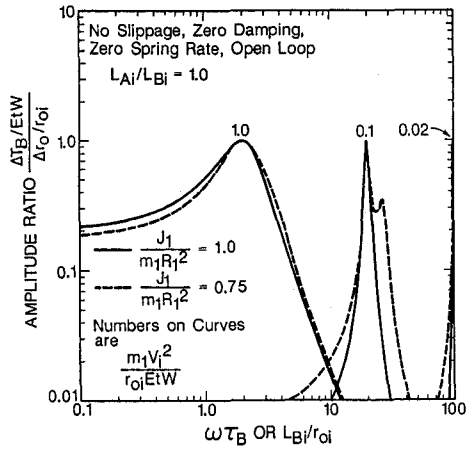

Fig. 13. Comparison of Tensions in Exiting Span for Dancer after Velocity-Controlled Unwind – with $J_1/m_1R_1^2$ = 0.75 and 1.0

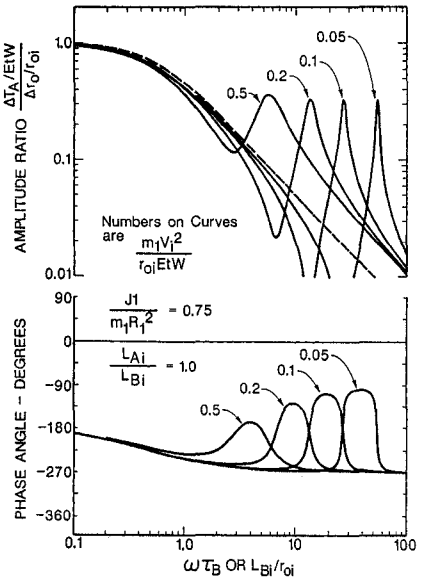

Fig. 14. Frequency Response of Span Upstream of Load-Cell Roller for Velocity-Controlled Unwind with Eccentric Roll (Open Loop, No Slippage)

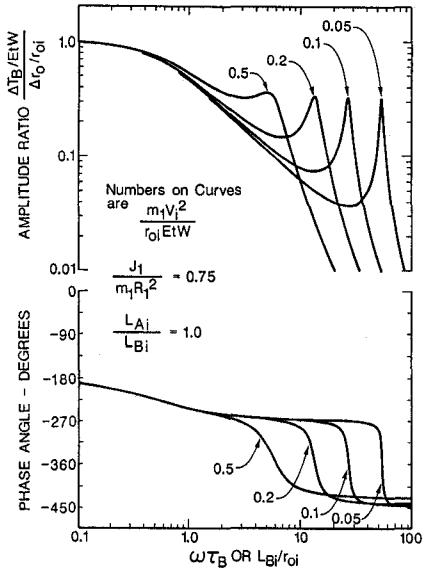

Fig. 15. Frequency Response of Span Downstream from Load-Cell Roller for Velocity-Controlled Unwind with Eccentric Roll (Open Loop, No Slippage)

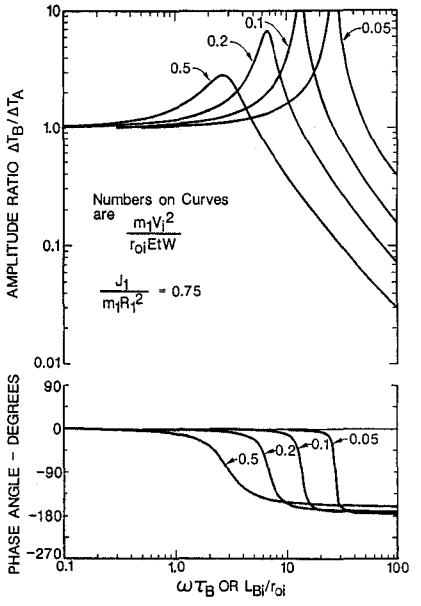

Fig. 16. Tension Ratio across Load-Cell Roller after Velocity-Controlled Unwind with Eccentric Roll (Open Loop, No Slippage)

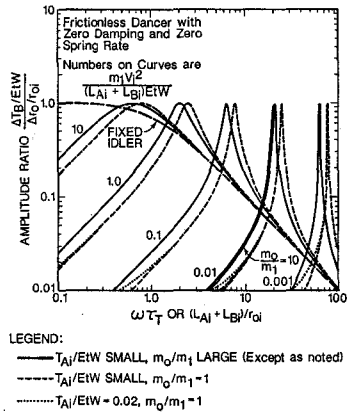

Fig. 17. Response of Tension to Unwinding Roll Eccentricity – Dancer after Torque-Controlled Unwind

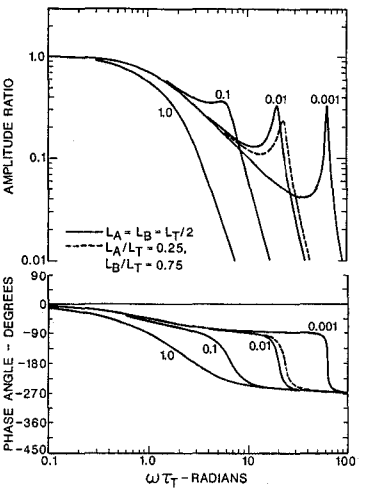

Fig. 18. One Idler – Response of ΔT_A to Downstream Input

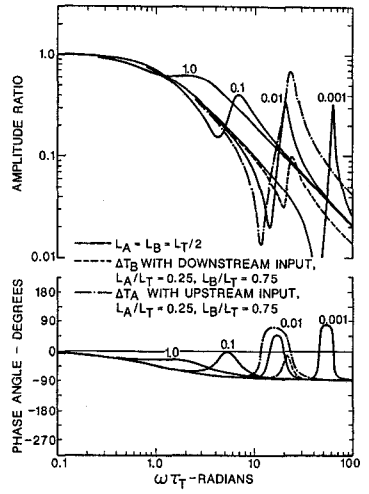

Fig. 19. One Idler – Response of ΔT_B to Downstream Input or ΔT_A to Upstream Input

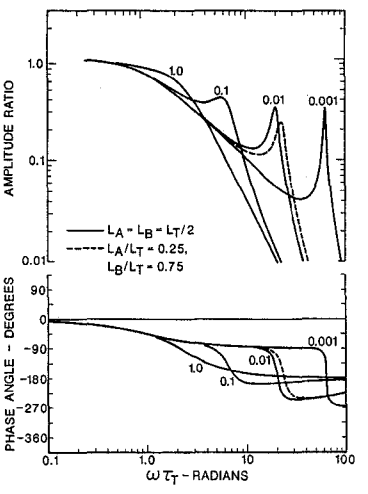

Fig. 20. One Idler – Response of ΔT_B to Upstream Input

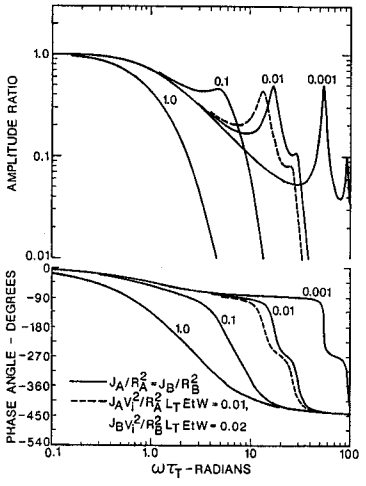

Fig. 21. Two Idlers – Response of ΔT_A to Downstream Input

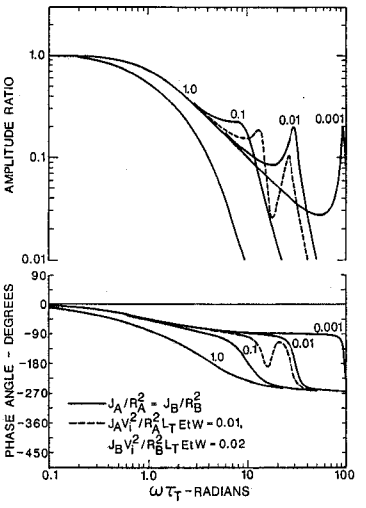

Fig. 22. Two Idlers – Response of ΔT_B to Downstream Input

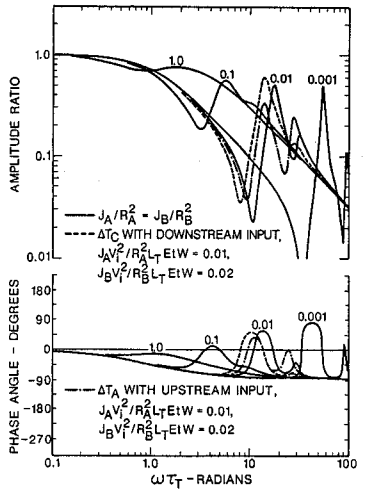

Fig. 23. Two Idlers – Response of ΔT_C to Downstream Input or ΔT_A to Upstream Input

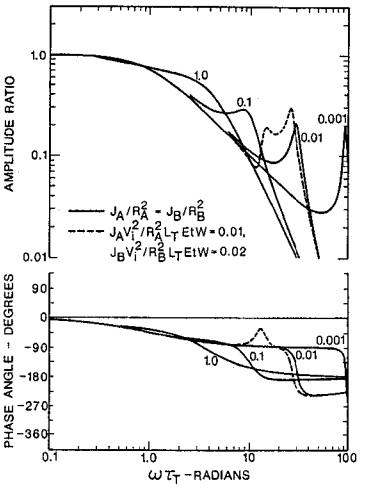

Fig. 24. Two Idlers – Response of ΔT_B to Upstream Input

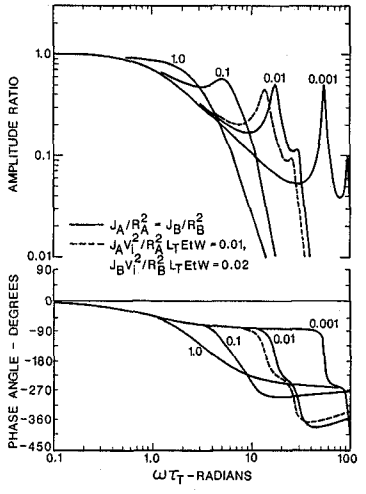

Fig. 25. Two Idlers – Response of ΔT_C to Upstream Input

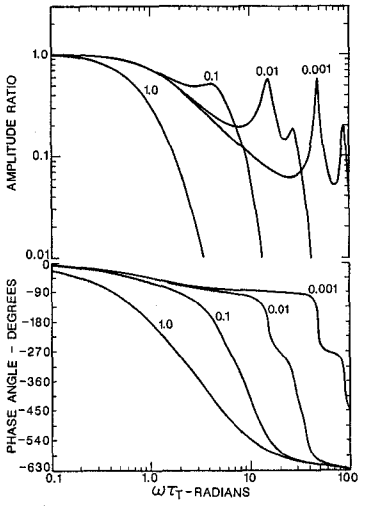

Fig. 26. Three Idlers – Response of ΔT_A to Downstream Input

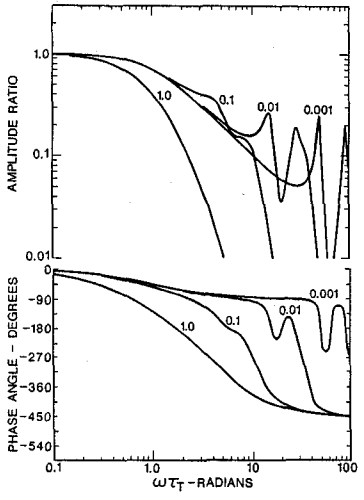

Fig. 27. Three Idlers – Response of ΔT_B to Downstream Input

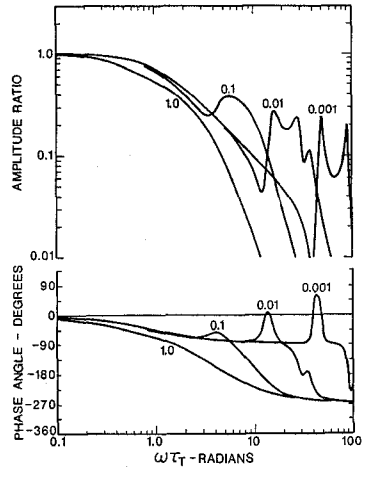

Fig. 28. Three Idlers – Response of ΔT_C to Downstream Input

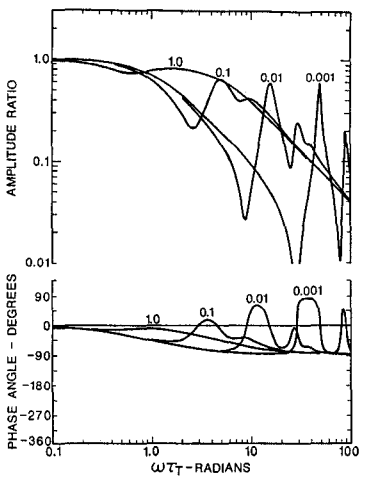

Fig. 29. Three Idlers – Response of ΔT_D to Downstream Input or ΔT_A to Upstream Input

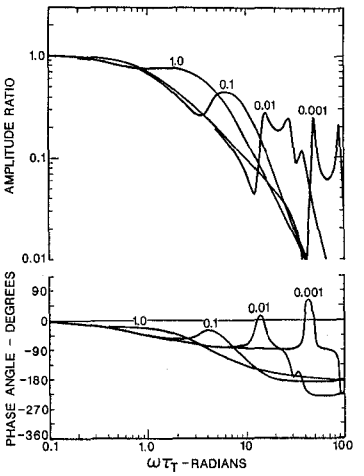

Fig. 30. Three Idlers – Response of ΔT_B to Upstream Input

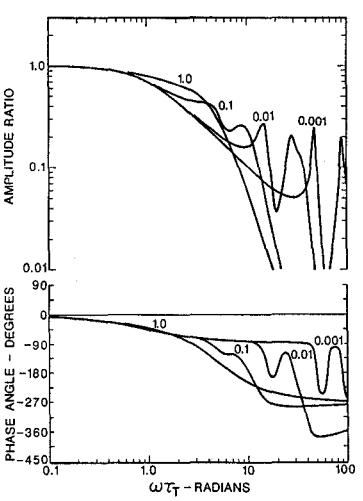

Fig. 31. Three Idlers – Response of ΔT_C to Upstream Input

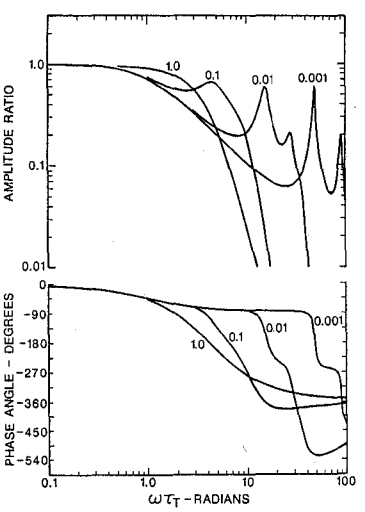

Fig. 32. Three Idlers – Response of ΔT_D to Upstream Input

J. J. Shelton
Limitations to Sensing of Web Tension by Means of Roller Reaction Forces
6/7/99 Session 1 1:25 – 1:50 p.m.

Question - Duane Smith, Black Clawson Co.
Did you do any work or do you have any plans for work on a large flywheel which changes the radius of gyration to equal the radius of the roller and see if tension variations are reduced at higher frequencies.

Answer – John Shelton, Oklahoma State University
My analysis compares a normal roller and an "inertia compensated" roller over a wide range of frequencies as shown in Figure 13. There is an improvement in variation of tension across the compensated dancer in a narrow band of frequency, but a deterioration in performance at other frequencies because of the added mass. For the compensated roller to reduce the variation of tension at any frequency, it must have adhesion to the web at all times, meaning that it must accelerate and decelerate at the frequency of the disturbance, not just rotate with its average surface velocity equal to the average velocity of the web.

We have no plans for experimental verification of the analysis of compensated versus uncompensated dancer rollers.